concept predict that the average concentration, $\overline{C}_X$, of an element X should depend on the particle diameter, d, according to an equation of the form (*10*)

$$\overline{C}_X = \overline{C}_0 + \overline{C}_A d^{-1}$$

where $\overline{C}_0$ is related to the average concentration of the element which is intrinsic to the particle and $\overline{C}_A$ is related to the average surface concentration added by adsorption or condensation. This equation relies on the poor assumption that particles of different sizes have the same bulk density. However, within the sampling and analytical errors reported, the model does predict the observed trends as illustrated in Fig. 1.

The model further predicts that trace metal concentrations should increase continuously with inverse particle diameter and that the surface concentration of the trace element should be greater than that in the particle interior. These predictions have been confirmed. Thus, Sparks (*11*) has shown that concentrations of the low-boiling (< 1600°C) elements Pb, Ba, Y, Sr, Rb, As, and Zn can be several orders of magnitude higher, in fly ash particles collected on a Millipore backup filter following a cascade impactor, than in those collected on the last impactor stage. The high-boiling elements Fe, Cu, and Ga did not show this effect. Scanning electron microscopic analyses by Hulett (*12*) of individual fly ash particles, which had been etched with a beam of argon ions, confirm that at least Ni, Cr, and Zn (the most concentrated elements listed in Table 1) are considerably more concentrated on particle surfaces than in their interiors.

In the case of sulfur, of course, it is hardly realistic to invoke a surface adsorption in view of the very high concentrations found in the small particle size fractions. These concentrations would suggest that some sulfur may be present as the element or as sulfide. This is contrary to the results of electron spectroscopy (*12*) which indicate the presence of sulfate. However, our sulfur analyses may be high owing to the possibility of preferential surface sampling by x-ray fluorescence and the associated calibration problems.

These results illustrate the importance of determining toxic trace element concentrations as a function of particle size if their full environmental impact is to be assessed. Furthermore, if the proposed volatilization-adsorption mechanism is basically correct, one would expect any high-temperature combustion source to produce concentration trends, similar to those reported here, for volatilizable species. Consequently, control technology designed to reduce the emission of toxic elements to the atmosphere should concentrate on the removal, or detoxification, of submicrometer-sized particles. In the latter context, preferential adsorption of volatile species onto large, easily collected particles of a heat-stable molecular sieve entrained with the feed air may provide an interesting and novel approach to the control of toxic element emissions.

D. F. S. NATUSCH
J. R. WALLACE
School of Chemical Sciences, University of Illinois, Urbana 61801
C. A. EVANS, JR.
Materials Research Laboratory, University of Illinois

References and Notes

1. H. A. Schroeder, *Environment (St. Louis)* **13**, 18 (1971).
2. B. L. Vallee and D. D. Ulmer, *Annu. Rev. Biochem.* **41**, 91 (1972).
3. R. E. Lee, Jr., and D. J. Von Lehmden, *J. Air Pollut. Control Ass.*, in press.
4. R. E. Lee, Jr., S. S. Goranson, R. E. Enrione, G. B. Morgan, *Environ. Sci. Technol.* **6**, 1025 (1972)
5. M. Kertesz-Saringer, E. Meszaros, T. Varkonyi, *Atmos. Environ.* **5**, 429 (1971); K. A. Rahn, R. Dams, J. A. Robbins, J. W. Winchester, *ibid.*, p. 413; P. R. Harrison, W. R. Matson, J. W. Winchester, *ibid.*, p. 613.
6. P. E. Morrow, *Am. Ind. Hyg. Ass. J.* **25**, 213 (1964); L. Dautrebande, *Microaerosols* (Academic Press, New York, 1962); M. Lippman and R. E. Albert, *Am. Ind. Hyg. Ass. J.* **30**, 257 (1969); *U.S. Dep. Health Educ. Welfare Publ. No. AP-49* (1969).
7. C. C. Patterson, *Arch. Environ. Health* **11**, 344 (1965).
8. Manufactured by the American Instrument Company, Anderson model 50-000.
9. A cascade impactor probe for operating at elevated temperatures inside the stack system.
10. D. F. S. Natusch, J. R. Wallace, C. A. Evans, Jr., in preparation.
11. C. J. Sparks, personal communication.
12. L. D. Hulett, personal communication.
13. Supported in part by NSF grants GI 31605 and GH 33634.

5 July 1973; revised 20 August 1973

Postseismic Viscoelastic Rebound

Abstract. *The sudden appearance of a dislocation, representing an earthquake, in an elastic layer (the lithosphere) overriding a viscoelastic half space (the asthenosphere) is followed by time-dependent surface deformation, which is very similar to in situ postseismic deformation. The spectacular postseismic deformation following the large Nankaido earthquake of 1946 yields for the asthenosphere a viscosity of* 5×10^{19} *poise and a 50 percent relaxation of the shear modulus. Large thrust type earthquakes may provide, in the future, a new method for exploring the rheology of the earth's upper mantle.*

A simple, widely accepted model for the mechanical behavior of the earth's crust and upper mantle consists of a relatively elastic, brittle lithosphere overlying a viscous, ductile asthenosphere. Evidence for the existence of the asthenosphere comes from the viscous rebound of the crust upon removal of surface loads, such as the postglacial uplift of Fennoscandia and the rebound of Lake Bonneville which followed the disappearance of the water load. The brittleness and elasticity of the lithosphere are implied by the abundance of crustal earthquakes and the associated elastic rebound.

In a strictly elastic earth, complete elastic rebound would take place in a few seconds and the only slow deformation would be the accumulation of tectonic strain. In contrast, in an earth with a viscous element, a large earthquake would consist of an initial elastic rebound followed by a transient element of deformation controlled by the viscosity.

In order to determine the characteristics of time-dependent deformation which follows the sudden slip on large earthquake faults, we consider the lithosphere-asthenosphere composite as an elastic layer overlying a viscoelastic half space (Fig. 1). Assuming that at time $t = 0$ sufficient tectonic stress has accumulated to cause sudden faulting, we obtain the solution to the elastic-viscoelastic model in two steps: first we solve for the static displacements and stresses due to a fault in an elastic layer welded to an elastic half space. We then make use of the correpondence principle and the Laplace transform to obtain the time-dependent solution.

Consider a two-dimensional elastic layer with shear modulus μ_1, bulk modulus K_1, and thickness H over an elastic half space with shear modulus μ_2 and modulus K_2. The surface $y_3 = 0$ is the free surface. In Fig. 1a we show the two types of faults that we consider here and for which we first determine the elastic solution. In the first case a strike slip fault is modeled by introducing at depth $y_3 = -D$ a screw dislocation with slip Δu (as shown in

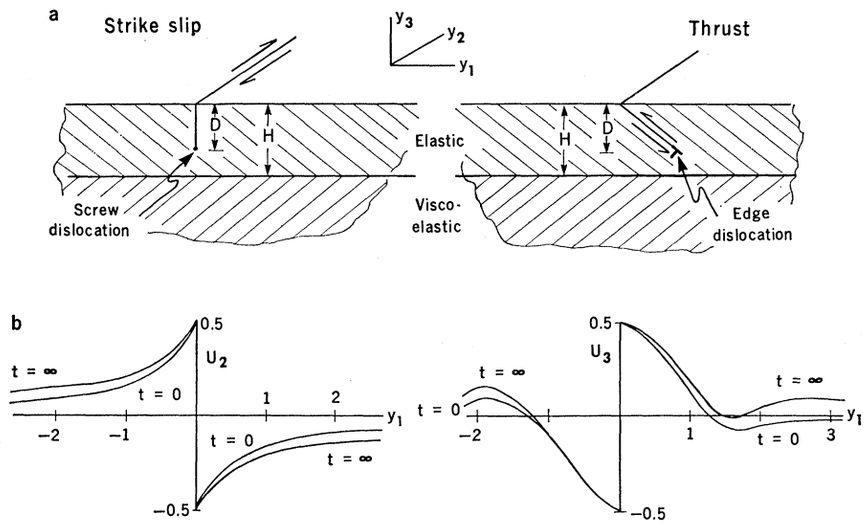

Fig. 1. (a) Simple models for earthquakes in an elastic lithosphere over a viscoelastic asthenosphere. A strike slip fault is modeled by a screw dislocation, and a thrust fault is modeled by an edge, introduced at $t = 0$. (b) The horizontal displacement for a screw and the vertical displacement for the thrust consist of a rapid initial part ($t = 0$) and a slow postseismic part, due to viscous relaxation of the asthenosphere. The time constant and the magnitude of the postseismic deformation are intimately related to the viscosity of the asthenosphere and the depth of faulting in the lithosphere, respectively.

Fig. 1a). The slip surface lies in the vertical plane $y_1 = 0$. The deformation associated with this dislocation is completely described by a single component of displacement U_2 (*1*) (and the two shear stresses σ_{12} and σ_{32}) and is given at the free surface $y_3 = 0$ by

$$U_2 = \frac{\Delta u}{\pi}\left\{\tan^{-1}\left(\frac{y_1}{D}\right) + \sum_{n=1}^{\infty}\left[\frac{\mu_1 - \mu_2}{\mu_1 + \mu_2}\right]^n\left[\tan^{-1}\left(\frac{y_1}{2nH + D}\right) - \tan^{-1}\left(\frac{y_1}{2nH - D}\right)\right]\right\} \quad (1)$$

In the second case, we model a thrust fault with an edge dislocation placed at depth D and with constant slip Δu. The slip plane, with dip ϕ, extends upward from the dislocation line in the positive y_3 direction. Here the deformation is described by the displacements U_3 and U_1 and the stresses σ_{33}, σ_{11}, and σ_{31}. The vertical displacement of the free surface ($y_3 = 0$) is given approximately (*2*) by

$$U_3 = \Delta u\left[\frac{f_1\left(1 - \frac{\mu_2}{\mu_1}\right)}{\left(1 + \frac{\delta_1\mu_2}{\mu_1}\right)} + \frac{f_2\left(\delta_2 - \frac{K_1\mu_2}{\mu_1}\right)}{\left(\delta_2 + \frac{\mu_2}{\mu_1}\right)} + f_3\right] \quad (2)$$

where f_i are geometric factors and $\delta_i = (3K_i + 7\mu_i)/(3K_i + \mu_i)$. The jump in displacement Δu for both faults is the offset on the slip plane. When $\mu_1 = \mu_2$, U reduces to the expressions for edge or screw dislocations in an elastic half space. When $\mu_2 = 0$, U describes the surface deformation of an elastic layer with an internal screw or edge dislocation.

Suppose now that the lower half space is viscoelastic. We use the correspondence principle (*3*) to obtain the slow, time-dependent deformation in response to the sudden deformation of a dislocation created at time $t = 0$. If the viscous behavior is due to a shear process, such as creep or relaxation of viscous fluid in pockets of melt, then only the shear modulus μ_2 must be replaced by the corresponding Laplace operator $\bar{\mu}$ for a standard linear viscoelastic solid

$$\bar{\mu}(s) = \frac{1}{2}\frac{b_0 + b_1 s}{a_0 + a_1 s}$$

where a_0, a_1, b_0, and b_1 are constants in the generalized relations between the shear stress σ_{ij} and the shear strain ε_{ij} ($i \neq j$)

$$\left(a_0 + a_1\frac{\delta}{\delta t}\right)\sigma_{ij} = \left(b_0 + b_1\frac{\delta}{\delta t}\right)\epsilon_{ij}$$

and s is the transform variable.

In order to obtain the complete viscoelastic solution, we introduce the initial conditions that either (i) Δu or (ii) the stress at some point on the slip plane is a step function in time. The Laplace transforms of these two conditions are

$$\bar{\Delta u}(s) = \frac{\Delta u}{s}$$

and

$$\bar{\sigma}_0(s) = \frac{\sigma_0}{s}$$

Substituting $\bar{\mu}$ and $\Delta\bar{u}$ into Eqs. 1 and 2 and taking the inverse Laplace transforms yields the time-dependent displacements at the free surface, as shown in Figs. 1b and 2. The sudden appearance of the edge dislocation produces initial surface displacement

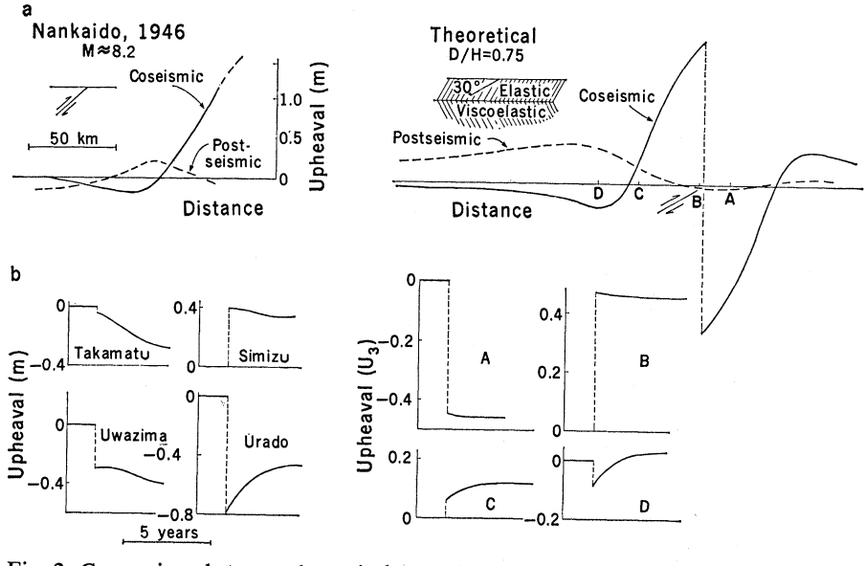

Fig. 2. Comparison between theoretical and observed seismic and postseismic deformation. (a) Spatial distribution of vertical displacements. In both cases coseismic and postseismic deformations are of comparable magnitude but of opposite signs in regions of largest rebound. (b) Vertical displacement time functions at selected neighboring points.

and tilts similar to values in an elastic half space. But, as time progresses, the deformation changes as a result of the relaxation of the shear modulus in the lower half space, as shown in Fig. 2a; the surface displacement spreads out away from the surface break, and the change with time of displacement at fixed points on the surface shows complicated patterns.

The duration of the slow transient deformation is characterized by the relaxation time constant τ for both screw and edge dislocations, given by the ratio of the viscosity η of the viscoelastic asthenosphere to the shear modulus μ_1 of the elastic lithosphere,

$$\tau = \alpha\eta/2\mu \ (1 < \alpha < 10)$$

Our models show that, if the asthenosphere is indeed viscous (and the lithosphere elastic), then crustal earthquakes with sufficiently deep faults should be followed by measurable postseismic deformation. The most spectacular example of such deformation was obtained after the Nankaido, Japan, thrust type earthquake (magnitude 8.2) of 20 December 1946.

In Fig. 2a we compare the results computed from a selected edge dislocation model (dip, 30°; depth, 0.75 of the crustal thickness) with the observed coseismic and postseismic deformation along a profile perpendicular to the surface break, reproduced from Kanamori (*4*). The computed and the observed initial coseismic vertical displacements are quite similar, both showing a zone of great uplift next to the fault and a broad zone of subsidence further away. The theoretical postseismic vertical displacement is obtained by subtracting the initial displacement from the final one, and the observed postseismic displacement is obtained from changes in beach levels during the 17-year period since the earthquake.

The similarity between the two postseismic curves is striking. In both most of the postseismic recovery takes place in the broad region of initial subsidence, and in both the amplitude of recovery is of the same order of magnitude as the initial amplitude of subsidence. This indicates that the postseismic deformation of the Nankaido earthquake results in all likelihood from viscous adjustments in the lower crust or the upper mantle of the earth.

In Fig. 2b we compare computed displacement time functions at selected points with observed vertical displacements measured at beaches on Shikoku Island (*4*). Both displacement sets show the initial, coseismic displacement followed by slow added deformation, and both sets show large, similar variation of these shapes over small horizontal distances.

The decay time τ for the observed deformation is of the order of 5 years. Taking an average crustal shear modulus $\mu_1 = 8 \times 10^{11}$ dyne/cm^2, $\tau = 1.6 \times 10^8$ seconds, and $\alpha = 5$, we obtain the viscosity $\eta = 5 \times 10^{19}$ poise. This value is in gratifying agreement, though not identical, with estimates based on very long viscous rebound from crustal loading in Fennoscandia and North America. The amplitude of the observed transient deformation indicates roughly a 50 percent relaxation of the shear modulus of the asthenosphere.

Because it is more difficult to measure horizontal displacements than vertical displacements, the data on relaxation after large strike slip earthquakes are rare. Nevertheless, several resurveys in Japan were probably precise enough to detect postseismic deformation although none was found. It is possible, therefore, that strike slip faults inherently fail to break to sufficient depth in the lithosphere to allow measurable postseismic deformation. Thrust faults, in contrast, probably break through almost the entire lithosphere.

The agreement between the postseismic data and the model, based on the current concepts of plate tectonics, provides not only an attractive explanation for postseismic deformation of shallow large earthquakes but also a new and independent confirmation that the asthenosphere behaves viscously, even over short periods of time. Careful monitoring of deformation after large earthquakes may provide a new tool for studying the upper mantle and may help to unravel the poorly understood physical processes responsible for its overall rheology.

AMOS NUR
GERALD MAVKO
Department of Geophysics,
Stanford University,
Stanford, California 94305

References and Notes

1. K. Rybicki, *Bull. Seismol. Soc. Am.* **61**, 79 (1971).
2. The exact solution for an edge dislocation parallel to the boundary of two joined elastic half spaces is given by T. Mura [in *Advances in Materials Research*, H. Herman, Ed. (Wiley, New York, 1968), vol. 3, pp. 1–108]. The free surface is approximated by considering two equal and opposite edge dislocations sharing a common slip plane, with the "free surface" midway between.
3. Y.-C. Fung, *Foundations of Solid Mechanics* (Prentice-Hall, Englewood Cliffs, N.J., 1965), p. 425.
4. H. Kanamori, *Annu. Rev. Earth Planet. Sci.* **1**, 213 (1973); T. Matuzawa, *Study of Earthquakes* (Uno Shoten, Tokyo, 1964).
5. This research was supported in part by a research fellowship from the Sloan Foundation (A.N.) and in part by a National Science Foundation fellowship (G.M.).

17 September 1973; revised 26 October 1973 ■

Ordered Lattice Defects in Colored Fluorite: Direct Observations

Abstract. *Ordered arrays of defect aggregates in the (111) planes of natural fluorite have been observed by transmission electron microscopy. The intense blue coloration observed in corresponding sample areas after 200-kilovolt electron microscopy confirms the conclusion that these are color-center aggregates and, conversely, that color centers are primarily responsible for fluorite coloration.*

The color and fluorescence of natural fluorite (CaF_2) have been the subject of many investigations over a period of more than a half century. Early summaries of fluorite studies indicated that the varying color of fluorite in deposits in the United States, South America, and Europe could be due to included organic matter or rare-earth compounds deposited on the surfaces of growing crystalline deposits (*1*). In a study of the ultraviolet absorption spectra of fluorite Titley and Damon (*2*) observed a strong absorption band at 3050 Å, and they ascribed a marked variation in the degree of absorption to a variable concentration of defects in the crystal structure. More importantly, Titley and Damon ascribed the absorption (coloration) characteristics to color centers similar to those outlined for the alkali halides in the classic papers by Seitz (*3, 4*).

The notion of color centers in minerals has been advocated by a number of investigators (*5, 6*), but, to my knowledge, there have been no reports of direct observations of any associated defect structure. Even in the review of Seitz (*4*), there were no reported incidents of direct observations of color centers in alkali halides, or of associ-